The Journal of the Textile Institute

Physical and compressional characteristics of a novel 3D fibrous structure - Application in comparison between PU foam and 3D fibrous structure

--Manuscript Draft--

Manuscript Number:	
Full Title:	Physical and compressional characteristics of a novel 3D fibrous structure - Application in comparison between PU foam and 3D fibrous structure
Article Type:	Research Paper
Keywords:	3D fibrous structure, PU foam, recycling, compression behavior
Corresponding Author:	Mouna Messaoud LPMT mulhouse, FRANCE
Corresponding Author Secondary Information:	
Corresponding Author's Institution:	LPMT
Corresponding Author's Secondary Institution:	
First Author:	Nicole Njeugna
First Author Secondary Information:	
Order of Authors:	Nicole Njeugna
	Laurence Schacher
	Dominique Adolphe
	Raphaël L. Dupuis
	Evelyne Aubry
	Jean-Baptiste Schaffhauser
	Patrick Strehle
	Mouna Messaoud
Order of Authors Secondary Information:	
Abstract:	The question of the recycling of the polyurethane (PU) foam, especially in the automotive industry represents one of the main technology thrust and challenge of the car manufacturers and the OEM (Original Equipment Manufacturer)'s since 2000. Indeed, it is nowadays necessary for car industry to promote ecological methods of development in regard to new consumer sensibility. New textile products present the best alternative solutions to answer this issue of replacement of the PU foam. Based on this fact, a new 3D fibrous structure made of polyester (PET) material has been developed in order to replace PU foam in automotive trim. These new manufactured 3D fibrous structures are laminated with needle-punched and spun-bonded sheets. The sheets are made of 100% PET in order to obtain a mono component product. Characterization of physical and mechanical properties of these new 3D fibrous structures, testing methods have to be developed. Based on the automotive specifications, a methodology has been set up to test the compression behavior of these new products. In order to answer the issue of replacement, some PU foam products have also been characterized and comparisons with the alternative products have been conducted. The results of this study show interesting properties of the new 3D fibrous structure in terms of compression behavior when compared to the PU foam.

Physical and compressional characteristics of a novel 3D fibrous structure - Application in comparison between PU foam and 3D fibrous structure

[1]Nicole Njeugna, [1]Laurence Schacher, [1]Dominique C. Adolphe, [2]Raphaël L. Dupuis, [2]Evelyne Aubry
[3]Jean-Baptiste Schaffhauser, [3] Patrick Strehle, [1] Mouna Messaoud

[1]ENSISA, Laboratoire de Physique et Mécanique Textile, Université de Haute Alsace, FR

[2]ENSISA, Modélisation Intelligence Processus Systèmes, Université de Haute Alsace, FR

[3]N. SCHLUMBERGER, FR

Correspondence to:
Mouna MESSAOUD, e-mail: mouna.messaoud@uha.fr

ABSTRACT
The question of the recycling of the polyurethane (PU) foam, especially in the automotive industry represents one of the main technology thrust and challenge of the car manufacturers and the OEM (Original Equipment Manufacturer)'s since 2000. Indeed, it is nowadays necessary for car industry to promote ecological methods of development in regard to new consumer sensibility. New textile products present the best alternative solutions to answer this issue of replacement of the PU foam. Based on this fact, a new 3D fibrous structure made of polyester (PET) material has been developed in order to replace PU foam in automotive trim. These new manufactured 3D fibrous structures are laminated with needle-punched and spun-bonded sheets. The sheets are made of 100% PET in order to obtain a mono component product.

Characterization of physical and mechanical properties of these new 3D fibrous structures, testing methods have to be developed. Based on the automotive specifications, a methodology has been set up to test the compression behavior of these new products. In order to answer the issue of replacement, some PU foam products have also been characterized and comparisons with the alternative products have been conducted. The results of this study show interesting properties of the new 3D fibrous structure in terms of compression behavior when compared to the PU foam.

Key words: 3D fibrous structure, PU foam, recycling, compression behavior

INTRODUCTION
Regarding the European directives 2000/53/CE [1] for recyclability and reusability, the automotive manufacturers have to redesign some multilayered materials used in car upholstery. In fact, all the products used in the automotive industry should be 85 % recyclable and 95 % re-useable by January 2015. This current research is taking place with this framework in mind.

The seat is the first visible component in the car interior and consequently one of the most important [2]. The traditional seat upholstery is a multilayered fabric usually composed of three layers (Figure 1). The top layer, mainly made of polyester (PET), is a decorative woven or knitted fabric. The second layer is a thin polyurethane (PU) foam with a thickness between 2 mm and 8 mm. The flexible foam used for the seat upholstery provides a comfort to the final multilayer through soft touch. The inner layer is usually a knitted fabric usually made of polyamide (PA) or polyester and used for mechanical stability [3].

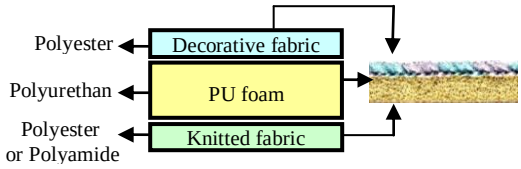

Figure 1.Composition of an automotive composite fabric

In terms of recyclability and environmental aspects, the PU foam layer is the main problem because of the delaminating process needed to separate the different layers. This operation is costly and presents a low efficiency in terms of purity of the products obtained. Indeed, some PU foam still remains on the PET fabrics. Moreover, some laminating process such as flame laminating generates toxic gases emissions [3, 4]. In such process, foam will be passed through an open flame whereby its surface will melt in order to serve as an adhesive. PU foams have many serious drawbacks such as flammability, gases emissions due to the laminating and delaminating processes [4]. These problems lead to the question of the replacement of the PU foam. A key aspect of the 3D new product is not to compromise the product functionality. It means that the new product should present, at least, mechanical properties closer or equal to the actual multilayered fabric ones. Another key aspect is to propose an environmental friendly solution presenting a mono material product. Moreover, this new product has to conform to the automotive specifications in terms of weight, formability, comfort and cost.

Our research project aims to develop a new 3D fibrous structure made of polyester material which

could be used in the car interior applications to replace PU foam. This new 3D structure could be laminated to different types of fibrous structure layers (needle-punched and spun-bonded). The laminated product, made of 100 % PET, will be able to replace the actual automotive multilayered fabric.

The paper will first focus on physical properties of the non-laminated and the laminated 3D fibrous structure products and foams. Then, a critical analysis of the compression behavior of these products will be carried out. Based on physical and mechanical characterization, a comparative study between the compression behavior of the new 3D fibrous structures and the PU foam will be highlighted. In order to characterize these new products, measurement methods and procedures have been developed and adapted.

1 MATERIALS AND METHODS

1.1 3D Nonwoven processing

The nonwoven products obtained from 3D technologies are well known as STRUTO®, WAVEMAKER®, NAPCO®, MALIMO or MALIVLIES [5, 6, 7].

In this work, a fiber-based product has been designed and developed in order to replace the PU foam in the composite fabric used in automotive industry for upholstery application. This new material is a pleated 3D fibrous structure. It is produced thanks to a new patented process called VERTILAP from the N. SCHLUMBERGER Company [8]. The VERTILAP process consists of a vertical lapping unit whereby a web of discontinuous fibers or a lap of continuous filaments is pleated to obtain a 3D structure [9].

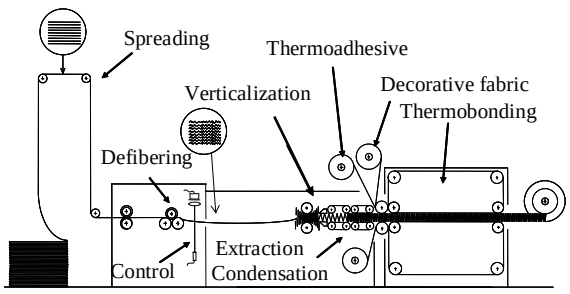

Figure 2.The VERTILAP process

In this paper, the manufacturing process has been carried out with an experimental prototype (Figure 2). The pleated 3D fibrous structures have been manufactured from a bicomponent polyester/copolyester tow. It is first defibred in order to individualize the filaments. Then, the defibered lap is verticalized and passed through a condensation area to condense the pleats. The tow has been manufactured under the glass transition temperature of the copolyester sheet which is 73 °C. Some of those single 3D fibrous structures have been laminated thanks to a flatbed laminating unit of the Meyer Company [10]. During this step, a thermo adhesive nonwoven, here a dry adhesive of 25 g /m^2 copolyester nonwoven is introduced to bind the single 3D fibrous structure and the laminating layers. The single 3D fibrous structure, the adhesive and the laminating layers are assembled and introduced in the system for heating. After heating, the materials are pressed together with the pressure rollers of the laminating unit. Then, they are guided through a cooling area. This process leads to thermal and mechanical stability of the multilayered structure. The most important parameters during the laminating process are the temperature, the pressure of the rollers and the speed of the belts. The pleated fibrous structure has been laminated either with a 40 g/m^2 needle-punched nonwoven or with a 44 g/m^2 spun-bonded nonwoven [11]. The top and the bottom of the multilayered structure are always composed of the same layer, i.e. needle-punched or spun-bonded nonwoven (Figure 3).

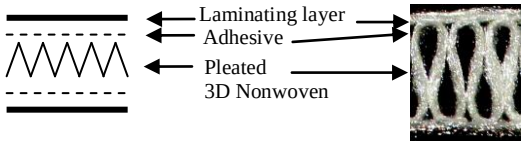

Figure 3. The 3D fibrous structure

1.2 Sample testing

All samples tested in this work are summarized in Table 1. The samples Nw1, Nw2, Nw3 and Nw4 represent the non-laminated 3D fibrous structures. The samples Nw1-N40 to Nw4-N40 are 3D fibrous structures laminated with the 40 g/m^2 needle-punched nonwoven and the samples Nw1-S44 to Nw4-S44 are the 3D fibrous structures laminated with the 44 g/m^2 spun-bonded nonwoven. The products A and B are

non-laminated foams and C is laminated foam (multilayered fabric).

	Non-laminated products		Laminated products	
Sample's codification	Nw1 Nw2 Nw3 Nw4	A B	Nw1-N40 to Nw4-N40 Nw1-S44 to Nw4-S44	C
Number of tested samples per product	31		15	31

Table 1. Samples listing

The physical and mechanical properties of 3D structures including their thickness, mass per unit area, geometrical modeling and compression behavior were investigated. The sample size for the characterization tests was 10 cm x 10 cm. The choice of these dimensions has been imposed by the initial width and the quality of the manufactured product of the experimental prototype.

1.3 Physical characterization

1.3.1 Thickness and mass per unit area

The thickness was measured via the KES-FB3 compression tester of the Kawabata Evaluation System for Fabrics. The measuring conditions were as follow: the sample is compressed under a load of 0.05 kPa and a speed of 12 mm/min. The mass is measured by a Mettler Toledo balance with a precision of 0.01 g.

1.3.2 Geometrical Modeling

The geometrical modeling includes the cell structure in the case of the foam. In the case of the 3D nonwoven, it includes the number of pleats per cm, the pleat's angle and the rate of pleats frequency.

Figure 4 shows that the cells of the foam can be geometrically modeled by a pentagon [12]. Based on adapted method from VISIOCELL® used by the OEM [13], the foam has been characterized by horizontal and vertical mean cell sizes. The measurement has been carried out with the image analysis software ImageJ®. The sizes are measured on different area of the sample and on a group of five adjacent cells. A minimum of 10 measures is taken on each sample.

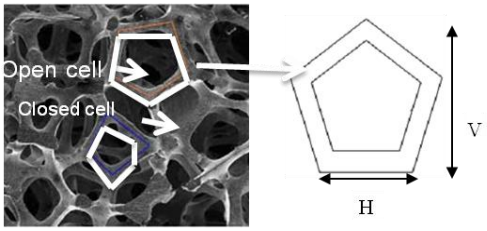

Figure 4. Modelling of the cell structure of the PU foam

In the case of the single 3D fibrous structure, the geometrical values of the pleats are used to characterize this new structure. Before condensation and lamination process, the pleat is geometrically modeled by a triangular shape (Figure 5). The thickness (e_0), the base's length (p) and the number of pleats (n_p) are measured in order to calculate the pleat angle (θ) (Equation 5), the pleat's hypotenuse (a) and the pleats frequency (T_x). T_x is calculated from the effective length (l_e) and the theoretical length (l_{th}) of the sample (Equation 1). The parameter l_{th} represents the length of the pleated sample and l_e represents the length of the sample when the pleated structure is opened. The effective length (Equation 2) is calculated from the base's length (p) (Equation 3), the hypotenuse (a) (Equation 4) and the theoretical length (l_{th}).

$$T_x(\%) = 100.\frac{l_e - l_{th}}{l_e} \quad (1)$$

$$l_e = 2.\frac{a.l_{th}}{p} \quad (2)$$

$$p = \frac{l_{th}}{n_p} \quad (3)$$

$$a = \sqrt{{e_0}^2 + \frac{P^2}{4}} \quad (4)$$

$$\theta = 2\arctan\frac{p}{2e_0} \quad (5)$$

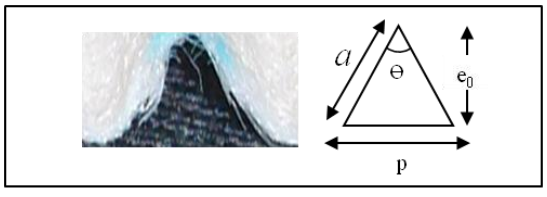

Figure 5. Modelling of the pleat before condensation and laminating steps

After condensation and laminating processing, the single 3D fibrous structure, the shape of the pleat is altered under the pressure rollers (Figure 6).

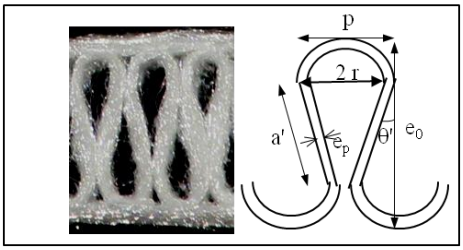

Figure 6. Modelling of the pleat after condensation and laminating steps

The new structure can be modeled by a loop and physical parameters schematically identified in Figure 6 are calculated as follows:

$$l_e = \pi.p + 2.a' \qquad (1')$$

$$l_{th} = n_p.l_e \qquad (2')$$

$$p = \frac{l_{th}}{n_p} = 2.r \qquad (3')$$

$$a' = \sqrt{(e_0 - p)^2 + \frac{p^2}{4}} \qquad (4')$$

$$\theta' = \arctan\frac{p}{2(e_0 - p)} \qquad (5')$$

1.4 Mechanical characterization

In order to characterize the mechanical properties of these new 3D fibrous structures, we have developed a procedure to evaluate the compression behavior. This procedure is based on the automotive standard ISO 3386/1:1986 [14] and has been customized in accordance with the recommendations of the Kawabata Evaluation System for Fabrics [15].

All the tests have been carried out on a universal screw driven testing machine (Instron 33R4204) fitted with 5 kN load cell. The compression speed has been chosen at 0.05 mm/s in accordance with the Kawabata recommendations [15] and automotive specifications [14]. The performed test is a static compressional one and the machine is equipped by two strictly parallel plate surfaces, i.e. a sliding plate (100 mm diameter) and a fixed plate (150 mm diameter) (Figure 7). The test procedure is the following: the sample is first compressed up to 50 % of its initial thickness then decompressed at the same speed until the plates are back to their initial positions. Then a 10 s wait in order to allow the sample to recover. This cycle is repeated 5 times. During the test, the time, the displacement and the load applied to the plate are measured.

Figure 7.Universal testing machine INSTRON 33R4204

2 RESULTS AND DISCUSSION

2.1 Physical characterization

The thickness, the mass per unit area, the cell mean size in the case of the foam, the pleat's angle and the pleat frequency in the case of the 3D fibrous structure will be successively presented and discussed as follow.

2.1.1 Thickness

Figure 8 presents the thickness of the tested products. It is mainly observed that the 3D fibrous structures samples are thicker than the foams. In the case of the foams, the laminated sample C is thinner than the non-laminated ones A and B. In fact, the initial foam used to obtain the final composite fabric (C) is thinner than the foams A and B. In the case of the 3D fibrous structures, the needle-punched laminated fibrous structures (Nw1-S44 to Nw4-S44) are lightly thicker than the non-laminated fibrous structures (Nw1 to Nw3) which are clearly thicker than the spun-bonded laminated fibrous structures (Nw1-N40 to Nw4-N40). This is due to the fact that a crushing phenomenon is observed during the lamination process (Figure 6). This buckling will be more important when using thinner laminating layers as the spun-bonded than when using needle-punched ones. There is no significant difference between the samples Nw1, Nw2 and Nw3.

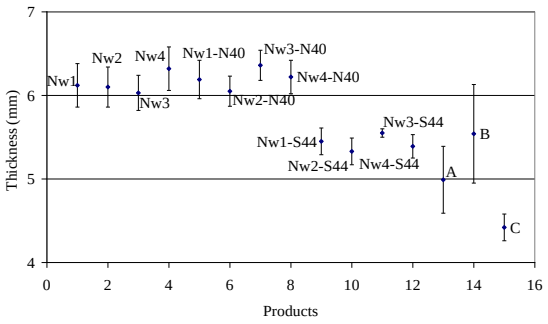

Figure 8.Product Thickness

2.1.2 Mass per Unit Area

Figure 9 presents the mass per unit area of the tested samples. It can be observed that the 3D fibrous structures materials are heavier than the foams and that, as expected the laminated products are heavier than the non-laminated ones. In particular, single fibrous structures (Nw1 to Nw4) are approximately 2.5 times heavier than foams A and B. For the same single 3D fibrous structure, the spun-bonded laminated fibrous structures are heavier than the needle-punched laminated ones. There is no significant difference between the couples of samples {Nw2; Nw4} and {Nw2; Nw3}.

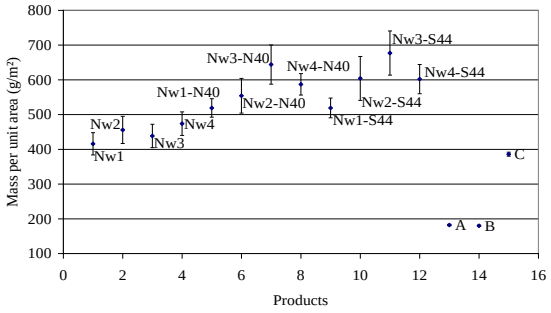

Figure 9. Mass per unit area of the tested products

2.1.3 Foams : Mean Cell Size

The cell size mean values of the tested foams are summarized in Figure 10. This parameter indicates if the cellular structure of the foam is opened or closed. Considering the horizontal cell mean size as the size close to the main cell diameter, it can be said that the foam A presents a closed cell structure while the foams B and C present an opened cell structure.

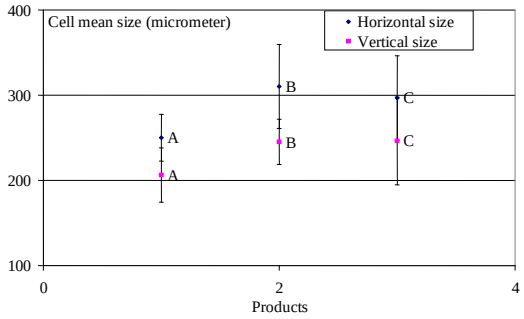

Figure 10. The cell mean size of the tested foams

2.1.4 Pleat's Angle

The pleat angle is measured using the Equation (5) for the non laminated 3D structures and using equation (5') for laminated ones. The values of the pleat's angle are illustrated in Figure 11. This physical parameter indicates the verticalization of the pleated nonwoven. That is to say if the fibers which composed the tow are more or less vertical. According to the geometrical modeling of the pleat, the value of the pleat angle should be close to 0° to reach the optimal vertical orientation before or after condensation and laminating steps. The characterization shows that the sample Nw4 is the most vertical and the sample Nw1 is the less vertical. There is no significant difference between the couples of samples {Nw2; Nw3} and {Nw2; Nw4}. After laminating, the sample Nw1 is more vertical than the sample Nw4. The two others present the same vertical characteristics.

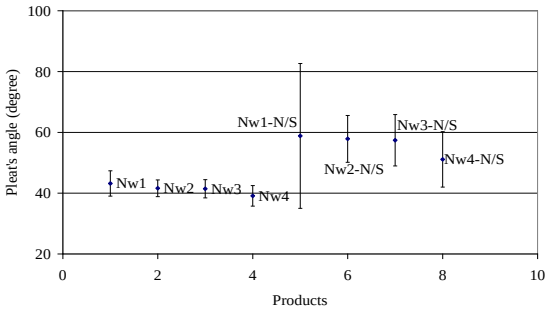

Figure 11. The pleat's angle of the 3D fibrous structure

2.1.5 Pleats Condensation Frequency

The values of the pleat condensation frequency of the tested 3D fibrous structures are presented in Figure 14. This parameter indicates the compactness of the pleated structure. It is observed that the sample Nw1 presents less compacted structure. There is no significant difference between the samples Nw2, Nw3 and Nw4. The two types of laminated fibrous

structures present the same compacted structure. So, it can be said that the type of laminating layer has no influence on this physical parameter.

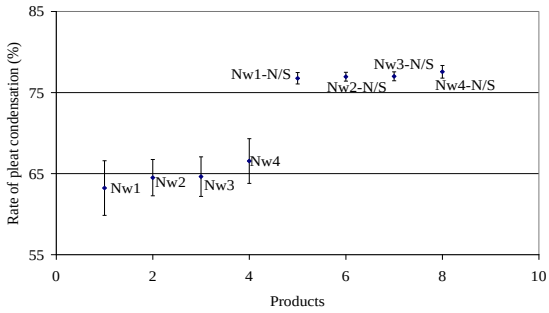

Figure 12. The rate of pleats condensation frequency of the 3D fibrous structure

2.2 Mechanical characterization

The load-displacement curves obtained during the compression test are studied for the different tested products. The maximum stress at 50 % of the deformation and the dissipated energy are analyzed.

2.2.1 Compression hysteresis

The Non-Laminated Products

Figures 13 to 15 display the compression behavior of the Nw3 sample, selected as an example of non-laminated 3D structure, the foam A (closed cell structure) and the foam B (opened cell structure), respectively. For various products, a significant difference can be observed between the 1st and the others cycles (2nd, 3rd, 4th and 5th). A permanent or delayed thickness deformation is observed after the 1st cycle therefore this deformation decreases slightly with repeated cycling. The 3D fibrous structures are more resistance to compression stress than the foams. But, the compression behaviour of the 3D fibrous structures is different compared to the PU foam, i.e. No plateau is identified in the case of the NW3.

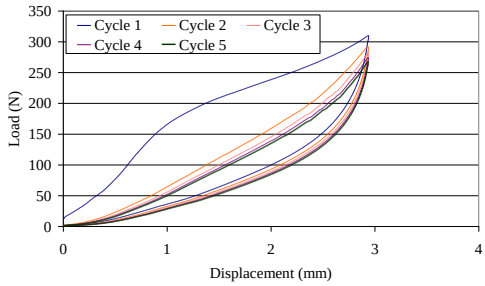

Figure 13.Load-displacement curve of sample Nw3

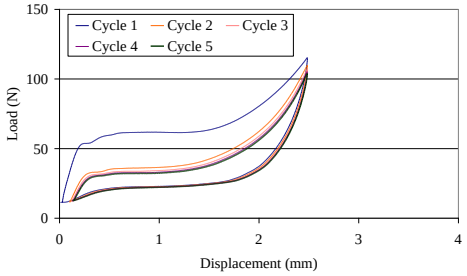

Figure 14. Load-displacement curve of foam A

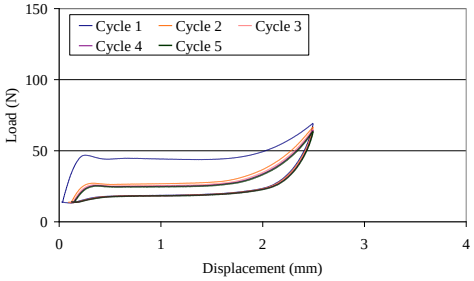

Figure 15. Load-displacement curve of foam B

In fact, the classical behavior of the PU foams is observed [16]. A linear elasticity at low strength is followed by a long collapse plateau. Then, a densification of the foam whereby a steeply rise of the stress is observed. A Plateau behavior is obtained but the mean value of this plateau decreases with the number of cycles and seems to tend to an asymptotic value. According to the cellular structure of the foams, the compression strength increases as the cell diameter decreases, and it decreases as the cell diameter increases. In the case of the foams A and B, the plateau behaviour decreases with the number of cycles but it does not tend to an asymptotic value.

During the compression test of all non-laminated samples, different steps of the compression behaviour are observed: the contact surface is first compressed followed by the buckling of the pleated structure. The hysteresis and the stabilisation are not reached after the 5th cycle. The existence of the compression hysteresis is due to the inter filaments friction.

The Laminated Products

The Figures 16 - 18 are displaying the compression behavior of the 3D fibrous structure Nw3-N40, Nw3-S44 and the laminated foam C. These graphs illustrate that the compression resistance of the laminated products closely approximate those of the non-laminated ones. It is also observed that under the same load the compressibility of the spun-bonded layers is lower than the needle-punched ones.

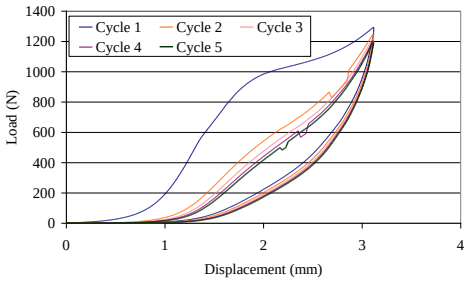

Figure 16.Load-displacement curve of the sample Nw3-N40

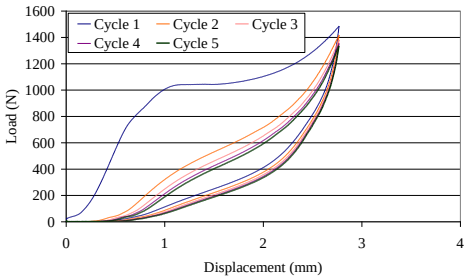

Figure 17.Load-displacement curve of the sample Nw3-S44

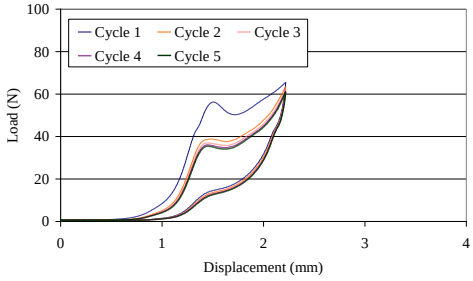

Figure 18.Load-displacement curve of the sample C

2.2.2 Dissipated/absorbed Energy

This parameter is related to the ability of the 3D material to absorb the energy applied. It can be observed that the 3D fibrous structures absorb more energy than the foams. As previously noticed, the 1st cycle presents higher value whatever the tested product is. The 3D fibrous structures absorb/dissipate 2-3 times more energy during this 1st cycle than the foams.

The Non-Laminated Products

Whatever the product is, we observe that the dissipated energy during the 1st cycle is twice larger than that dissipated during the 2nd cycle. This phenomenon highlights the reorganization process of the internal structure within the material during the 1st cycle.

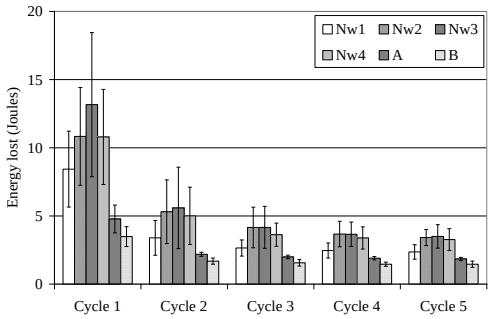

Figure 19.The dissipated energy of the non-laminated products

Regarding the 3D fibrous structures, the difference in value between the 1st and 2nd cycles is hugely marked. This discrepancy can be explained by the reorganization of the fibrous structure in the 3D nonwoven and the energy lost due to inter fiber friction. From the 2nd cycle of compression, the energy tends to stabilize and this stabilization is clearly observable from the 4th cycle. Based on Figure 19 and statistical analysis comparing averages between the different cycles, the following ranking could be done in terms of stabilization; the sample Nw1 followed by samples Nw2, Nw3 and Nw4. The sample Nw1 is beginning to stabilize from the 3rd cycle, while it was not until the 4th cycle to observe a clear stabilization for other fibrous structures. By the same way, the following ranking could be extracted in terms of energy dissipation; samples Nw2 and Nw3 following by samples Nw4 and Nw1.

Regarding the foams, it can be observed that the foam A dissipates more energy than foam B. The collapse of cells in the expulsion of air of the foam A stabilizes the deformation energy at the 4th cycle. This could be explained by the structure of closed cellular foam A.

A large variation of results has been found for 3D fibrous structures. So, it can be said that the foams seem to have a more reproducible compression behavior compared to 3D fibrous structures.

The Laminated Products

The laminated 3D fibrous structures dissipate largely more energy than the non-laminated ones (Figure 20). We observe that the dissipated energy during the 1st cycle is twice larger than that dissipated during the 2nd cycle except for the multilayered fabric C (Figure 21). The laminated 3D nonwoven with the spun-bonded dissipates more energy than those laminated with the needle-punched.

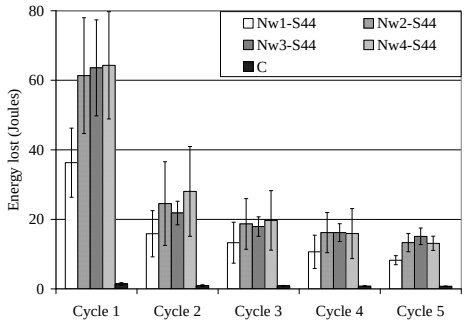

Figure 20.The dissipated energy of the laminated 3D fibrous structures Nwi-N40 and the multilayered fabric C

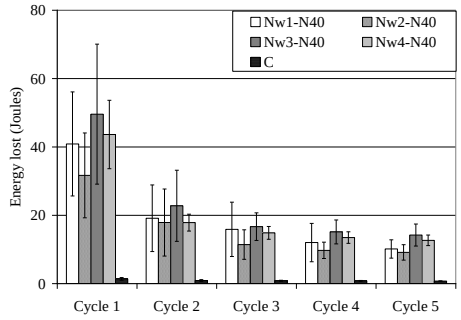

Figure 21.The dissipated energy of the laminated 3D fibrous structures Nwi-N40 and the multilayered fabric C

2.2.3 Maximum Stress Applied at 50% of Initial Thickness Deformation

This parameter represents the resistance of the material to the compression solicitations and it is called "lift". It is commonly accepted [17] that greater the strength required to compress the foam, greater the foam is called "lifting". And as the "lift" parameter is correlated to the comfort, the fabric having the more important lift parameter will be more comfortable [17]. Contrary to the previous observations, the difference between the 1st and the other cycle is, here, very slight; nevertheless this difference is statistically significant. For this parameter, the 3D fibrous structure highlights a better resistance to compression than the tested foams. This fact has to be mentioned as an advantage in regard to future use of this material in automotive industry.

The Non-Laminated Products

The Figure 22 shows that the samples Nw1 and Nw2 begin to stabilize their resilient behavior after the 3rd cycle. The resilient behavior of the samples Nw3 and Nw4 stabilize at the 5th cycle while the foam A stabilizes after the 4th cycle. Foam B has the same resilient behavior whatever the number of cycle is. Overall the 3D fibrous structures present maximum load values at 50 % of the initial thickness deformation 2-3 times higher than those for tested foams. It can be concluded that they are more resilient in compression and thus more comfortable than foams.

Concerning the foams, we can notice that the foam A is more resistant to compression than foam B, so foam A is more comfortable than foam B. It can be also concluded that the samples Nw2 and Nw3 are more comfortable than the samples Nw1 and Nw4. These results can be explained via the analysis of their physical characteristics. Indeed, the sample Nw1 presents less compacted structure (lowest rate of pleats condensation) and the most opened one (highest pleat's angle). Similarly, samples Nw2 and Nw3 show better physical characteristics than sample Nw1. Regarding sample Nw4, in spite of its better physical characteristics, its poor strength could be explained by poor regularity of the structure.

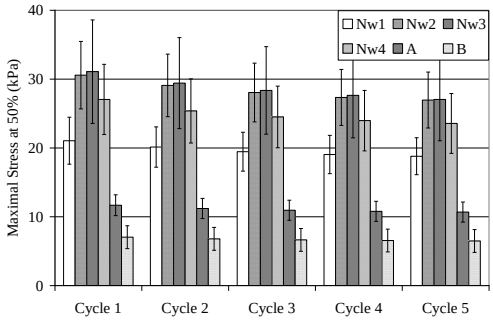

Figure 22.Maximum stress at 50% of initial thickness deformation of the non-laminated products

The Laminated Products

Figure 23 shows that the laminated 3D fibrous structures are 5 times more resistant to compression stress than the non-laminated ones. They are also more resistance than the composite fabric C. The laminated 3D structures obtained with spun-bonded are less compressible than those laminated with the needle-punched. The dispersion values show that the foam has less variability than the 3D fibrous structures.

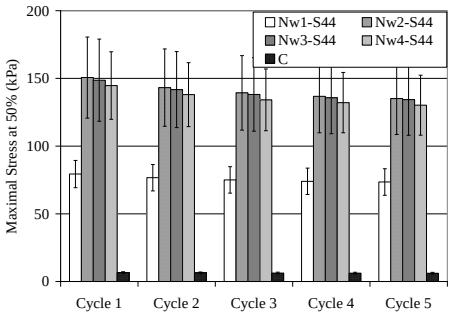

Figure 23.Maximum stress at 50% of initial thickness deformation of laminated samples Nwi-S44 and C

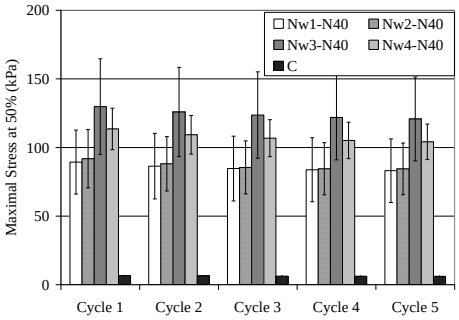

Figure 24.Maximum stress at 50% of initial thickness deformation of laminated samples Nwi-N40 and C

CONCLUSIONS

A new product has been developed in order to satisfy the new European Directives of recyclability and reusability for automotive industry. In this study, new 3D fibrous structures (with or without lamination) were produced with a patented verticalization process. These products have been tested using newly developed procedures and compared with three foams usually used in automotive industry.

The physical and geometrical parameters of the foam samples have less variability than the 3D fibrous structures. Indeed, the 3D fibrous structures are manufactured from an experimental prototype that is still under development. In addition, as produced 3D fibrous structures are characterized by heterogeneity of the filament density due to the opening process of the feeding tow.

Based on physical characterization results of the non-laminated and laminated products, the foams are lighter and thinner than the 3D fibrous structures. The mass per unit area of the 3D fibrous structures has to be decreased through the manufactured process during further investigations in order to fulfil automotive standards. Based on our results, it can be concluded that the foams B and C, characterized by an opened cellular structure, are more recommended for seat upholstery application while the closed cellular structure, foam A, can be suitable for door panel upholstery application.

Compression Behaviour analysis indicates that the 3D fibrous structures are more resilient than the foams materials and they dissipate more energy. This can be explained by the fact that the vertical orientation of the fibers has the effect to provide maximum resilience to the material and lead to the reorganization of the fibrous structure under compression stress. It also highlights the relationship between the compressive mechanical behavior of these materials and their physical characteristics (values and dispersion). In addition, the laminating process reinforces the 3D structure and increases its compression performance. Based on energy dissipation evaluation, we can conclude that the 3D fibrous structures laminated with the spun-bonded would be more comfortable than those laminated with the needle-punched and a good candidate to replace foam.

In conclusion, all these results underline the ability of the new pleated structure material to substitute polyurethane foam to obtain sustainability. In spite of their interesting mechanical properties, these new 3D fibrous structures have to be improved. In fact, their reproducibility and their mass per unit area should be improved in order to reach the key points of regularity and lightness. Other samples and tests have to be performed in order to increase the regularity and to decrease the mass per unit area by using a nonwoven fabric as a raw material. This study still under progress and new finding will be presented in subsequent article.

BIBLIOGRAPHIC REFERENCES

[1] Directive 2000/53/CE du parlement Européen et du conseil du 18 septembre 2000 relative aux véhicules hors usage, Journal officiel des Communautés européennes (2000).

[2] Fung, W & Hardcastle, M. (2001). Textiles in automotive engineering. In A Woodhead Publishing Limited in association with The textile Institute (195).

[3] Caudron, J-C. (2003). Etude du marché du polyuréthane et Etat de l'art de ses techniques de recyclage. Agence de l'Environnement et de la Maîtrise de l'Energie (ADEME).

[4] Hopkins, J. (1995). A comparative analysis of laminating automotive textiles to toam. Journal of coated fabrics, 24, 250-267.

[5] STRUTO® Nonwoven, Struto International Inc, http://www.struto.com/

[6] WAVEMAKER® Nonwoven, Santex Group, http://www.cavitec.ch/en/?menu=produkteprogramm

[7] The Karl Mayer guide to Technical Textiles, Karl Mayer Group, http://www.karlmayer.com/

[8] Dumas, J-L. & Schaffhauser, J-B. (2007). N. SCHLUMBERGER company, patent N° WO2007125248.

[9] Njeugna, N., Adolphe, D.C., Schacher, L., Schaffhauser, J-B., & Strehle, P. (2008). Modification of compressional testing procedures for 3D nonwoven system for automotive interior applications, Book of proceedings of the 4th International Textile Clothing & Design Conference, (pp 859-863), ISBN 978-953-7105-26-6, October 5th to 8th 2008, Dubrovnik, Croatia.

[10] Flatbed laminating system of the Meyer Company, Maschinen Fabrik Herbert Meyer GmbH, Germany, www.meyer-machines.com

[11] Njeugna, N., Adolphe, D.C., Schacher, L., Schaffhauser, J-B., & Strehle, P. (2008). 3D nonwoven system for automotive interior applications, Textile & plastics. 6th International Conference on Automotive and Transport Interior Decoration, Dec'autex 2008, Mulhouse, France.

[12] Drean, E. (2006). Contribution au développement de capteurs piézoélectriquees pour la caractérisation mécanique des étoffes, Université de Haute Alsace, France.

[13] Recticell (1999). Anew method to measure the cell diameter of polyurethane foam, viocell technical foams. Business line management technical foams (Edition 1), pp 4-8, DAMSTRAAT, BELGIUM

14] ISO 3386/1 : 1986, Polymeric materials, cellular flexible–Determination of stress-strain characteristics in compression – Part 1 : Low density materials (1986).

[15] Kawabata S., « The standardization and analysis of hand evaluation » 2nd ed., The Textile Machinery Society of Japan, Osaka (1980)

[16] Bouchou, A., Gontier, C. & Vinot, C. (1999). Modélisation du comportement en compression d'une mousse phénolique, Matériaux et Techniques, 11-12, 10-15.

[17] Sauniere, J., Timbre, A. (2003). Flexible foam padding made from melamine and applications thereof, patent W0/2003/072391.